Conformations, Unfolding, and Refolding of Apomyoglobin in Vacuum: An Activation Barrier for Gas-Phase Protein Folding

Konstantin B. Shelimov[†] and Martin F. Jarrold*

Contribution from the Department of Chemistry, Northwestern University, 2145 Sheridan Road, Evanston, Illinois 60208

Received August 19, 1996[⊗]

Abstract: Gas-phase ion mobility measurements have been used to characterize the conformations of the +4 to +22 charge states of apomyoglobin. For the +8 to +10 charge states, generated by electrospraying pH ≈3 solutions, two relatively compact conformations were resolved which may reflect the state of the protein in solution. These relatively compact conformations unfold into more extended conformations when collisionally heated. Only extended conformations are observed for the high (>+10) charge states, and they become more extended as the charge increases. Proton stripping of the higher (>+7) charge states to produce the +4 to +7 charge states results in spontaneous collapse into partially folded conformations. Further folding is observed upon collisional heating of the collapsed structures, indicating the presence of an activation barrier for protein folding in the gas phase. The barrier probably results from Coulomb repulsion and the reorganization of secondary structure. For the lower (<+7) charge states, the most stable conformations appear to be slightly more compact than the native protein in solution. The collision cross sections per residue for the extended conformations of apomyoglobin and cytochrome *c* are similar. The cross sections for the compact folded conformations of these proteins also scale with the number of residues. This suggests that different proteins share common structural motifs in the gas phase, as they do in solution.

Introduction

Intramolecular hydrogen bonding[1] and hydrophobic interactions[2] have long been recognized as the major factors responsible for the stability of biologically active protein conformations. However, the relative importance of these and other factors is still a subject of controversy. It has been argued that the hydrophobic effect makes the dominant contribution to protein stability[3] and that this effect is small and perhaps even destabilizing.[4] Estimates of the stabilization energy due to intramolecular hydrogen bond formation range from 50 to −6.3 kJ mol^{-1}.[5,6] Thus it is not surprising that attempts to separate protein folding energetics into intramolecular and hydration contributions using different methods produce inconsistent results. For example, two recently reported estimates of the folding enthalpy of several proteins in vacuum, from experimental solution values[7] using the accessible surface area model of solvation[8] and from molecular mechanics modeling using the CHARMM force field,[9] differ by an average of 10.5 kJ mol^{-1} per residue. This is more than an order of magnitude larger than a typical free energy of protein folding in solution. It is clear that the free energy of protein folding in solution involves a near cancellation of several large contributions. Before one can hope to predict the relative energies of various protein conformations in solution, one has to be able to determine the magnitude of the individual contributions with a much higher accuracy. Thus an independent test of stability of protein conformations in a solvent-free environment is required. This test can be provided by studying protein conformations in the gas phase. Studies of this type can also help to refine theoretical models of the intramolecular interactions in proteins. To understand how a protein folds, it is necessary to have reliable molecular mechanics force fields. The presence of the solvent in biological systems greatly complicates the development of such force fields. In most theoretical models the solvent is accounted for by either introducing non-uniform dielectric constants or by explicitly including solvation shells in the simulations. If structural information was available for biomolecules in the gas phase, the development and testing of force fields would be greatly facilitated.

Since the development of gentle ionization techniques that can put large biomolecules into the gas phase,[10,11] there has been a considerable interest in studying protein conformations in vacuum. Obtaining structural information about gas-phase proteins is a challenging problem. Indirect methods such as H/D exchange studies and proton transfer kinetics have been employed,[12−14] along with more direct probes such as the kinetic energy loss in ion beam scattering experiments[15−17] and the examination of the shapes of the defects produced by the impact of protein ions on surfaces.[18] Ion mobility measurements[19] can provide direct information about the conformations of protein

[†] Present address: Department of Chemistry, Rice University, Houston, TX 77251.

[⊗] Abstract published in *Advance ACS Abstracts,* March 15, 1997.

(1) Mirsky, A. E.; Pauling, L. *Proc. Natl. Sci. U.S.A.* **1936**, *22,* 439.
(2) Kauzmann, W. *Adv. Protein Chem.* **1959**, *11,* 14.
(3) Dill, K. A. *Biochemistry* **1990**, *29,* 7133.
(4) Privalov, P. L.; Gill, S. J. *Adv. Protein Chem.* **1988**, *39,* 193.
(5) Makhatadze, G. I.; Privalov, P. L. *J. Mol. Biol.* **1993**, *232,* 639.
(6) Yang, A.-S.; Honig, B. *J. Mol. Biol.* **1995**, *252,* 351.
(7) Privalov, P. L. *Adv. Protein Chem.* **1979**, *33,* 167. Privalov, P. L. *Annu. Rev. Biophys. Chem.* **1989**, *18,* 47.
(8) Makhatadze, G. I.; Privalov, P. L. *Adv. Protein Chem.* **1995**, *47,* 307.
(9) Lazardis, T.; Archontis, G.; Karplus, M. *Adv. Protein Chem.* **1995**, *47,* 231.
(10) Karas, M.; Hillenkamp, F. *Anal. Chem.* **1988**, *60,* 2299.
(11) Meng, C. K.; Mann, M.; Fenn, J. B. *Z. Phys.* **1988**, *10,* 361.
(12) Wood, T. D.; Chorush, R. A.; Wampler, F. M.; Little, D. P.; O'Connor, P. B.; McLafferty, F. W. *Proc. Natl. Acad. Sci. U.S.A.* **1995**, *92,* 2451.
(13) Cassady, C. J.; Carr, S. R. *J. Mass Spectrom.* **1996**, *31,* 247.
(14) Gross, D. S.; Schnier, P. D.; Rodriguez-Cruz, S. E.; Fagerquist, C. K.; Williams, E. R. *Proc. Natl. Acad. Sci. U.S.A.* **1996**, *93,* 3143.
(15) Covey, T. R.; Douglas, D. J. *J. Am. Soc. Mass Spectrom.* **1993**, *4,* 616.
(16) Collins, B. A.; Douglas, D. J. *J. Am. Chem. Soc.* **1996**, *118,* 4488.
(17) Cox, K. A.; Julian, R. K.; Cooks, R. G.; Kaiser, R. E. *J. Am. Soc. Mass Spectrom.* **1994**, *5,* 127.
(18) Quist, A. P.; Ahlbom, J.; Reimann, C. T.; Sundavist, B. U. R. *Nucl. Instrum. Methods Phys. Res. B* **1994**, *88,* 164.

S0002-7863(96)02914-9 CCC: $14.00

ions in the gas phase. The mobility of a polyatomic ion, how fast it moves through a buffer gas under the influence of a weak electric field, depends on its geometry; thus different conformations can be separated. Collision cross sections can be determined from the mobilities, and then information about the geometries can be obtained by comparing the cross sections to those calculated for trial geometries. Recently, von Helden et al. have used this approach to analyze the conformations of ethylene glycol oligomers and the nonapeptide bradykinin.[20,21] Work in our group has focused on studies of larger biomolecules.[22] We have recently reported a systematic study of the conformations of bovine pancreatic trypsin inhibitor (BPTI) and cytochrome *c* in the gas phase as a function of charge.[23,24] Gas-phase BPTI retains its compact solution-phase conformation, probably because it has three disulfide bridges. Cytochrome *c*, on the other hand, undergoes a sharp unfolding transition as its charge is increased, presumably in response to Coulomb repulsion. Multiple conformations were observed for several charge states of cytochrome *c*.

In the present paper we report a systematic study of the gas-phase conformations of the +4 to +22 charge states of another globular protein, apomyoglobin. Like cytochrome *c*, apomyoglobin is a relatively small protein (153 residues) that does not have any disulfide bridges and thus it is free to adopt preferred gas-phase conformations. The types of conformations observed for gas-phase apomyoglobin are compared to those observed in our previous studies of cytochrome *c*. The folded and extended conformations of the two proteins are similar on a collision cross section per residue basis. On the other hand, for apomyoglobin there are clearly substantial activation barriers for folding in the gas phase.

Experimental Methods

The injected ion drift tube apparatus used in the studies reported here has been described in detail previously.[23,25] Solutions of horse heart myoglobin (Sigma Chemical Co.) in a 3:1 mixture of water and acetonitrile were electrosprayed in air. The protein concentration was typically 2×10^{-5} M, and the solutions were usually acidified with 0.25% acetic acid. The solution flow rate was ~0.2 mL/h and the needle was operated at 5 kV. Ions enter the first chamber of the apparatus, a desolvation/proton-stripping region, through a 0.012-cm aperture. The pressure in this region is typically around 0.1 Torr. The desolvation region can be heated to 200 °C. A 2−30 V retarding potential increases the time ions spend in this region. Charge states of +8 and above were generated by direct electrospray ionization. Lower charge states were obtained through proton stripping of the higher charge states in the desolvation region[12,26] by high proton affinity bases: 3-(dimethylamino)propylamine (DMAPA, gas-phase basicity GB = 229.4 kcal/mol[27]) and 1,3,4,6,7,8-hexahydro-1-methyl-2*H*-pyrimido-[1,2-*a*]pyrimidine (MTBD, GB = 243.3 kcal/mol[28]) both obtained from Aldrich Chemical Co. The pressure of the base in the desolvation region was below 10^{-3} Torr. The proton stripping reactions were normally carried out with the desolvation region at 150 °C, while studies that did not employ a base were usually performed with the desolvation region at room temperature.

After exiting the desolvation region, ions are focussed into the first quadrupole mass spectrometer of the tandem quadrupole injected ion drift tube apparatus.[25] Short (15−50 μs) pulses of ions were selected by applying a voltage pulse, at a frequency of 375 Hz, to the deflection plates in front of the quadrupole. The ions of interest were mass selected by the quadrupole and injected into the drift tube. The drift tube contains helium buffer gas at around 2.5 Torr. If the injection energy is high enough, the transient collisional heating that occurs as the ions enter the drift tube can drive conformational changes. The ions then travel slowly across the drift tube under the influence of a 13.2-V/cm electric field. Conformations with different shapes have different drift times and are separated. After the ions exit the drift tube, they can be mass analyzed by the second quadrupole mass spectrometer. They are then detected with an off-axis collision dynode and dual microchannel plates. Drift time distributions were recorded with a multichannel scaler.

The drift time distributions provide information about the number of isomers present and their relative abundances. The drift times can be converted into collision cross sections using the expression:[29]

$$\sigma = \frac{(18\pi)^{1/2}}{16}\left[\frac{1}{m}+\frac{1}{m_b}\right]^{1/2}\frac{ze}{(k_B T)^{1/2}}\frac{t_D E}{L}\frac{1}{N} \qquad (1)$$

where m and m_b are the masses of the ion and the buffer gas respectively, ze is the charge of the ion, t_D is the drift time, E is the electric field, L is the length of the drift tube, and N is the buffer gas number density. The collision cross sections derived in this way can be used to deduce structural information about the ion, as described in detail below.

Mobility Calculations

Structural information is deduced from ion mobility measurements by calculating cross sections for trial geometries and comparing them to the measured values. In most of the previous ion mobility studies, the cross sections were estimated using a projection approximation which is based on determining the orientationally averaged geometric cross section.[30,31] However, the cross sections obtained from ion mobility measurements are really collision integrals that should be calculated by averaging the momentum transfer cross section over relative velocity and collision geometry.[29,32] The momentum transfer cross section depends on the scattering angles between the incoming and outgoing trajectories in collisions between the polyatomic ion and the buffer gas atoms. In order to determine the scattering angle it is necessary to define a realistic intermolecular potential and perform trajectory calculations.[33] An enormous number of trajectories must be run to average over the impact parameter, collision geometry, and relative velocity, and for protein ions containing thousands of atoms

(19) Hagen, D. F. *Anal. Chem.* **1979**, *51*, 870. Karpas, Z.; Cohen, M. J.; Stimac, R. M.; Wernlund, R. F. *Int. J. Mass Spectrom. Ion Proc.* **1986**, *83*, 163. von Helden, G.; Hsu, M. T.; Kemper, P. R.; Bowers, M. T. *J. Chem. Phys.* **1991**, *95*, 3835. Jarrold, M. F.; Constant, V. A. *Phys. Rev. Lett.* **1992**, *67*, 2994. For a recent review see: St. Louis, R. H.; Hill, H. H. *Crit. Rev. Anal. Chem.* **1990**, *21*, 321.

(20) von Helden, G.; Wyttenbach, T.; Bowers, M. T. *Science* **1995**, *267*, 1483.

(21) Wyttenbach, T.; von Helden, G.; Bowers, M. T. *J. Am. Chem. Soc.* **1996**, *118*, 8355.

(22) Clemmer, D. E.; Hudgins, R. R.; Jarrold, M. F. *J. Am. Chem. Soc.* **1995**, *117*, 10141.

(23) Shelimov, K. B.; Clemmer, D. E.; Hudgins, R. R.; Jarrold, M. F. *J. Am. Chem. Soc.* **1996**, *118*, 2240.

(24) Shelimov, K. B.; Jarrold, M. F. *J. Am. Chem. Soc.* **1996**, *118*, 10313.

(25) Jarrold, M. F.; Bower, J. E.; Creegan, K. *J. Chem. Phys.* **1989**, *90*, 3615. Jarrold, M. F.; Bower, J. E. *J. Chem. Phys.* **1992**, *96*, 9180.

(26) Schnier, P. D.; Gross, D. S.; Williams, E. R. *J. Am. Chem. Soc.* **1995**, *117*, 6747.

(27) Lias, S. G.; Liebman, J. F.; Levin, R. D. *J. Phys. Chem. Ref. Data* **1984**, *13*, 695.

(28) Decouzon, M.; Gal, J. F.; Maria, P. C.; Raczynska, E. D. *Rapid Commun. Mass Spectrom.* **1993**, *7*, 599.

(29) Mason, E. A.; McDaniel, E. W. *Transport Properties of Ions in Gases*; Wiley: New York, 1988.

(30) Clemmer, D. E.; Hunter, J. M.; Shelimov, K. B.; Jarrold, M. F. *Nature* **1994**, *372*, 248. Hunter, J. M.; Fye, J. L.; Jarrold, M. F.; Bower, J. E. *Phys. Rev. Lett.* **1994**, *73*, 2063. Hunter, J. M.; Jarrold, M. F. *J. Am. Chem. Soc.* **1995**, *117*, 10317. Jarrold, M. F. *J. Phys. Chem.* **1995**, *99*, 15. Shelimov, K. B.; Clemmer, D. E.; Jarrold, M. F. *J. Chem. Soc., Dalton Trans.* **1996**, 567.

(31) von Helden, G.; Hsu, M.-T.; Gotts, N.; Bowers, M. T. *J. Phys. Chem.* **1993**, *97*, 8182. von Helden, G.; Gotts, N. G.; Maitre, P.; Bowers, M. T. *Chem. Phys. Lett.* **1994**, *227*, 601. von Helden, G.; Wyttenbach, T.; Bowers, M. T. *Int. J. Mass Spectrom. Ion Proc.* **1995**, *146/147*, 349. Lee, S.; Wyttenbach, T.; von Helden, G.; Bowers, M. T. *J. Am. Chem. Soc.* **1995**, *117*, 10159.

(32) Hirschfelder, J. O.; Curtis, C. F.; Bird, R. B. *Molecular Theory of Gases and Liquids*; Wiley: New York, 1954.

(33) Mesleh, M. F.; Hunter, J. M.; Shvartsburg, A. A.; Schatz, G. C.; Jarrold, M. F. *J. Phys. Chem.* **1996**, *100*, 16082.

this consumes large amounts of computer time. In an effort to reduce the computer time required to estimate the collision cross sections for large polyatomic ions we have recently developed an exact hard spheres scattering model.[34] This model treats the scattering process between the ion and buffer gas correctly, within the hard sphere limit, but ignores the effects of the long-range interactions. Cross sections determined with the exact hard spheres scattering model for the native conformations of BPTI and cytochrome *c* are within 1% of the cross sections determined by trajectory calculations.[35] On the other hand, cross sections for BPTI and cytochrome *c* determined using the projection approximation deviate by over 20% from the values determined by trajectory calculations, because the projection approximation ignores the details of the scattering process between the polyatomic ion and the buffer gas. Thus, it appears that the exact hard spheres scattering model provides a reasonably efficient way of estimating the collision cross sections for these large protein ions, and this approach was employed here. The implementation of the exact hard spheres scattering model requires empirical values for the hard sphere contact distances between the buffer gas and the atoms in the protein. As described previously,[24] the hard sphere contact distances for the heavy atoms in the protein were all taken to be 2.7 Å, and the hard sphere contact distance for hydrogen was taken to be 2.2 Å. The collision cross section determined for the native conformation of myoglobin[36] with the exact hard spheres scattering model is 1768 Å^2. The average collision cross section calculated for an α-helical form, obtained by setting all Φ angles to −57° and all Ψ angles to −47°, is 3258 Å^2, and the average collision cross section for a string-like conformation obtained by setting all backbone torsion angles to 180° is 4944 Å^2.

The calculations described above were performed with rigid geometries. And while the results provide useful limiting values for comparison with the experimental data, the geometries of the protein ions are dynamic, to some extent, as they travel through the drift tube. To account for this behavior it is necessary to perform molecular dynamics simulations of the protein ion and then average the collision cross section over the geometries sampled. This approach has been employed by Book et al.[37] and Wyttenbach et al.[21] for much smaller systems. We are not yet able to perform these calculations for protein ions of the size considered here. An assumption with all of the calculations described above is that the collisions are elastic. The increase in the effective temperature due to the drift field is typically less than a degree Kelvin,[38] and the protein ions are in thermal equilibrium with the buffer gas, except for a short time immediately after injection into the drift tube when they are cooling down after being collisionally heated. If the protein ions are in thermal equilibrium with the buffer gas then *on average* the collisions are elastic. There have not yet been any studies to determine how inelastic collisions, where energy is transferred both into and out of relative kinetic energy, affect the mobility of a polyatomic ion.

Experimental Results

Electrospray ionization generates protonated protein ions in a distribution of charge states that depends on the acidity of the electrosprayed solution. In our apparatus the distribution can be modified by adding a base to the desolvation region, so that proton stripping reactions reduce the charge state. By adjusting the conditions, a wide variety of charge states can be produced, as illustrated in Figure 1. The mass spectra shown in this figure were obtained by electrospraying myoglobin from a pH ≈3 solution. The mass spectrum in Figure 1b was obtained by adding MTBD to the desolvation region, while no base was added for the spectrum in Figure 1a. In both cases the most prominent peaks in the mass spectra are in positions that correspond to multiply protonated ions of apomyoglobin,

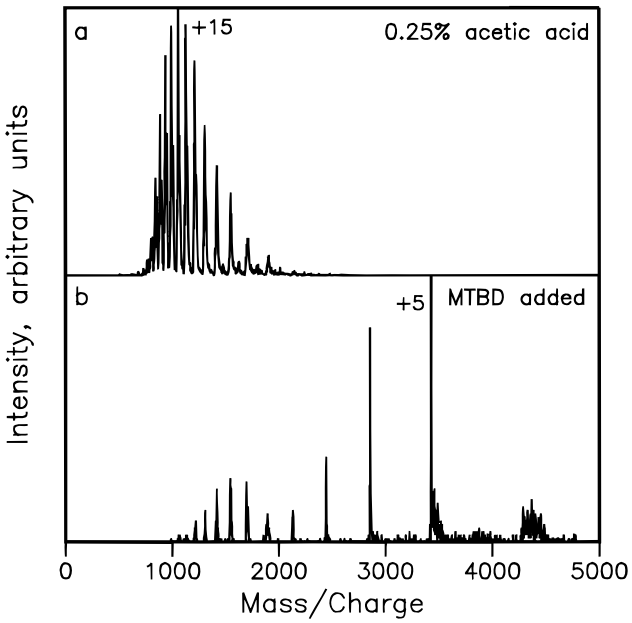

Figure 1. Mass spectra recorded for apomyoglobin electrosprayed from a solution acidified with 0.25% acetic acid. For part (b) MTBD was added to the desolvation region. The additional peaks for the +4 and +5 charge states in part (b) are due to the addition of MTBD molecules to the protein ions.

i.e. myoglobin devoid of the heme group. In myoglobin the heme group is not covalently bound in the heme pocket and it can be easily detached from the protein by an acid or a denaturant. It has previously been observed that myoglobin electrosprayed from acidic solutions lacks the heme group.[39] Most of the ion mobility studies described below were performed for apomyoglobin.

By changing the conditions in the electrospray source and the desolvation region the most abundant charge state can be varied from +16, as in Figure 1a, to +5, as in Figure 1b. Increasing the solution acidity leads to the formation of higher charge states as a result of increased proton concentration and the increase in the accessible surface area due to denaturation.[40] On the other hand, increasing the base pressure in the desolvation region shifts the charge distribution toward lower charge states. The protein ions also undergo addition reactions with the base. The number of base molecules attached to the protein ions increases with decreasing charge (see the +4 and +5 charge states in Figure 1b). Along with multiply protonated apomyoglobin monomers, lower-intensity peaks attributable to protein dimers can be seen in Figure 1a. Dimers with an odd number of charges have mass/charge ratios that lie half way between the more abundant monomer peaks. The abundance of the dimers increases with decreasing charge. On the other hand, almost no dimers are seen in Figure 1b where base was added to the desolvation region.

Figure 2 shows drift time distributions for the +8 charge state of apomyoglobin recorded as a function of the injection energy. The results shown in the figure were obtained by electrospraying a pH ≈3 solution without a base in the desolvation region. The dashed line in the figure corresponds to the drift time determined for myoglobin in its native conformation using eq 1 and the cross section obtained using the exact hard spheres scattering model. At low (200−600 eV) injection energies two broad peaks are observed. The left peak has a drift time that is slightly

(34) Shvartsburg, A. A.; Jarrold, M. F. *Chem. Phys. Lett.* **1996**, *261*, 86.
(35) Shvartsburg, A. A.; Jarrold, M. F. Unpublished results.
(36) Evans, S. V.; Brayer, G. D. *J. Mol. Biol.* **1990**, *213*, 885.
(37) Book, L. D.; Xu, C.; Scuseria, G. E. *Chem. Phys. Lett.* **1994**, *222*, 281.
(38) The effective temperature increase due to the drift field is given by $m_B V_D^2/3k_B$, where v_D is the drift velocity, m_B is the mass of the buffer gas atom, and k_B is Boltzmann's constant.[30]
(39) Feng, G.; Konishi, Y. *Proceedings of the 40th ASMS Conference on Mass-Spectrometry and Allied Topics*; Washington, DC, 1992.
(40) Chowdhury, S. K.; Katta, V.; Chait, B. T. *J. Am. Chem. Soc.* **1990**, *112*, 9012.

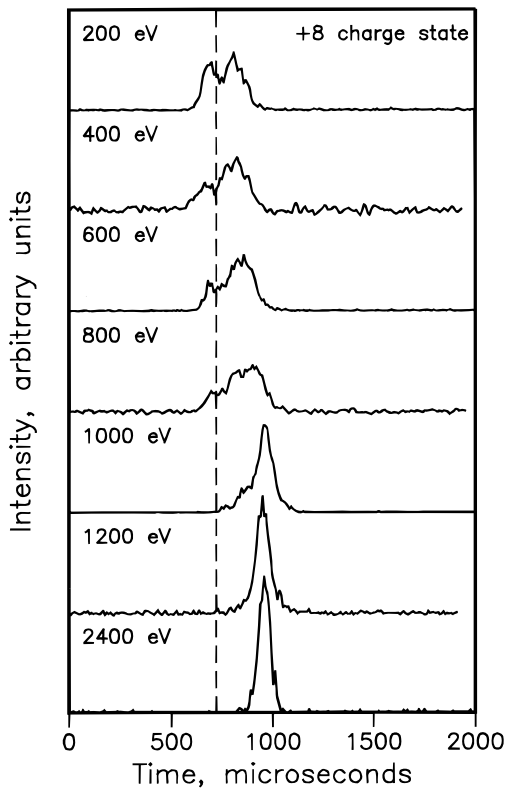

Figure 2. The drift time distributions recorded for the +8 charge state of apomyoglobin at injection energies of 200−2400 eV. The +8 charge state was obtained from a pH ≈3 solution by direct electrospray ionization. The dashed line shows the drift time estimated for the native conformation of myoglobin using eq 1 and the cross section calculated using the exact hard spheres scattering model.

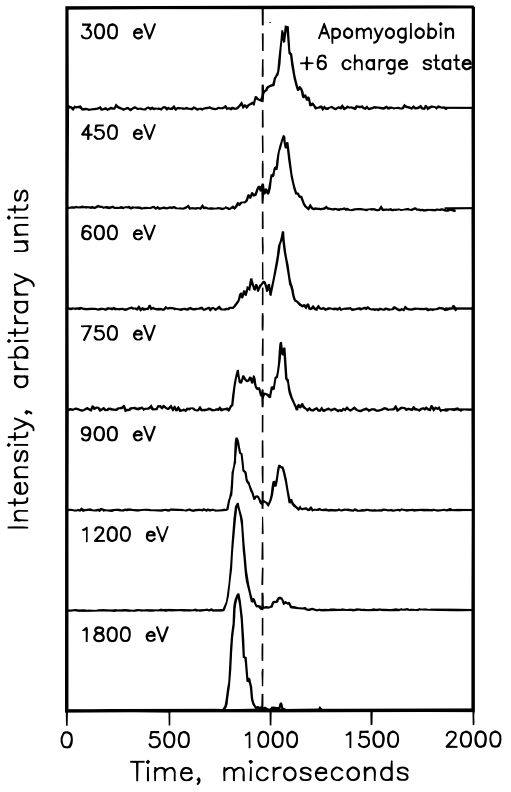

Figure 3. The drift time distributions recorded for the +6 charge state of apomyoglobin at injection energies of 300−1800 eV. The +6 charge state was obtained by proton stripping from higher (>+7) charge states. The dashed line shows the drift time estimated for the native conformation of myoglobin using eq 1 and the cross section calculated using the exact hard spheres scattering model.

shorter than expected for native conformation, indicating that the conformation(s) responsible for this peak are slightly more compact than the native form. The two conformations resolved at low injection energies are stable enough to survive on the millisecond time scale of the experiment. However, substantial structural changes occur as the injection energy is raised. First, the peak at shorter drift times decreases in intensity, and then the peak at longer drift times appears to gradually shift to the right. This transformation apparently proceeds through a series of similarly-shaped, unresolved conformations. Between injection energies of 800 and 1000 eV the broad feature in the drift time distributions transforms into a relatively narrow peak with a longer drift time than any of the original conformations. As the injection energy is increased to 1200 eV, the remainder of the broad feature disappears and the narrow peak at 970 μs becomes the only feature in the drift time distribution. The drift time distribution does not change further as the injection energy is raised to 2400 eV. No fragmentation products attributable to the dissociation of the parent apomyoglobin monomer were observed in mass spectra recorded with the second quadrupole mass spectrometer, even at the highest injection energies employed. Thus the changes in the drift time distributions are due to the gradual unfolding of the initial conformations into less compact structures. Unfolding processes similar to those described above were also observed for the +9 and +10 charge states obtained through direct electrospray ionization. For the +11 to +22 charge states, we have recorded drift time distributions at injection voltages of 100−150 V, which corresponds to high injection energies for these charge states. Studies were not performed as a function of injection energy for the high charge states. The distributions show a single narrow peak which correlates with the most extended conformations of the +8 to +10 charge states.

Different behavior is observed when lower charge states are generated by proton stripping of higher charge states. Since the high charge states of apomyoglobin have extended conformations, the low charge states are initially unfolded and then may fold into lower-energy compact structures. Figure 3 shows the drift time distributions recorded for the +6 charge state of apomyoglobin. These ions were produced by electrospraying a pH ≈3 solution and proton stripping with DMAPA. Similar results were obtained with MTBD. Charge states above +10 dominate in the mass spectrum generated by electrospraying a pH ≈3 solution, while charge states below +7 constitute a negligible fraction of the charge distribution (see Figure 1). With DMAPA added to the desolvation region, only the +6, +7, and +8 charge states remain in the mass spectrum. The drift time distribution recorded for the +6 charge state at low (300 eV) injection energy (see Figure 3) is dominated by a single peak. The drift time of this peak is substantially longer than that expected for the native conformation of myoglobin, shown by the dashed line in the figure. However, the drift time is substantially shorter than expected for the extended high charge state conformations. Thus after proton stripping in the desolvation region, a substantial amount of folding occurs, presumably without, or with a low, activation barrier. The folding stops when the protein reaches the conformation observed in the drift time distribution at 300 eV. As the injection energy is raised and the protein is collisionally heated, further folding occurs. Ultimately a folded structure that is slightly more compact than the native protein is formed (see the drift time distributions in Figure 3 recorded with the injection energies of 1200−1800

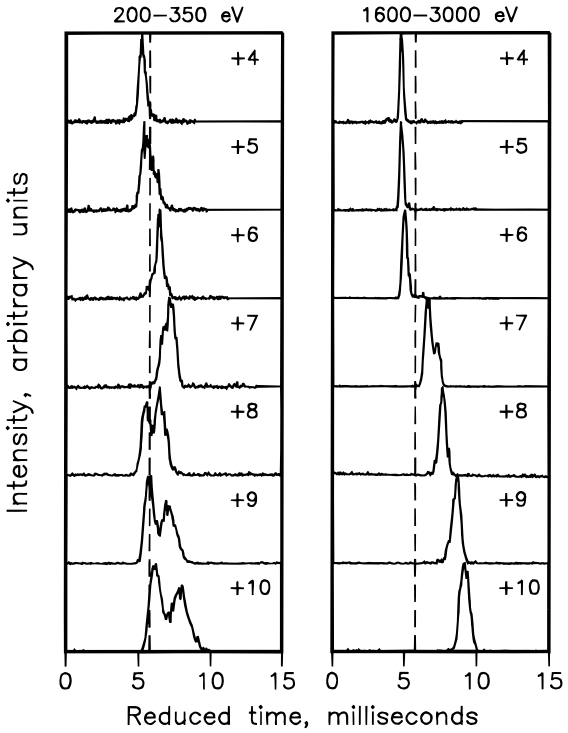

Figure 4. Drift time distributions recorded for the +4 to +10 charge states of apomyoglobin at low (200−350 eV) injection energies (on the left) and high (1600−3000 eV) injection energies (on the right). The ions were produced by electrospraying a pH ≈3 solution. The +4 to +7 charge states were obtained by proton stripping of higher charge states. The +8 to +10 charge states were generated by direct electrospray ionization. The reduced drift times were obtained by multiplying the measured drift times by the charge. The dashed line shows the drift time estimated for the native conformation of myoglobin using eq 1 and the cross section calculated using the exact hard spheres scattering model.

eV). This transformation seems to proceed through at least two intermediates, although the intermediates are poorly resolved.

Figure 4 shows drift time distributions recorded for the +4 to +10 charge states of apomyoglobin under different conditions. The measured drift times have been multiplied by the charge to obtain a charge independent time scale. The dashed lines in the figure show the reduced drift time expected for the native conformation. The distributions on the left were recorded for apomyoglobin electrosprayed from a pH ≈3 solution at low (200−350 eV) injection energies. The +8 to +10 charge states were obtained by direct electrospray ionization. The +4 to +7 charge states were generated through proton stripping of higher charge states. The right-hand side of Figure 4 shows drift time distributions recorded at high injection energies. These distributions do not depend on how a particular charge state was produced. At low injection energies an array of folded and partially folded structures is observed for the +4 to +6 charge states. These structures result from the collapse of the extended conformations of the higher charge states. Upon collisional heating, the peaks narrow and the partially folded structures convert into conformations that are slightly more compact than the native form. The folded conformations become slightly less compact with increasing charge.

At the +7 charge state, there is an abrupt change in the drift time distributions. Conformations slightly more compact than the native form no longer dominate at high injection energies. Instead, two peaks are observed at slightly longer drift times than expected for the native conformation. The low injection energy peaks for the +7 charge state are close to those observed

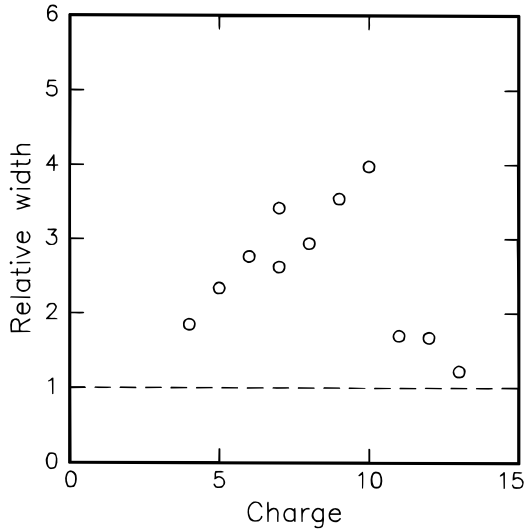

Figure 5. The relative widths (fwhm) of the peaks in the high-injection-energy drift time distributions for the +4 to +13 charge states of apomyoglobin. The relative widths were obtained by dividing the measured width by the width calculated for a single conformation.

at high injection energies, although they still undergo noticeable changes during collisional annealing. For the +8 to +10 charge states, generated by direct electrospray ionization, two peaks are observed at low energies. Both peaks are broad and must consist of several slightly different conformations. Annealing of the +8 and all higher charge states results in the formation of a single narrower peak at longer drift times. This peak gradually shifts to longer drift times with increasing charge.

Figure 5 shows the relative widths of the peaks (fwhm) observed in the drift time distributions at high injection energies plotted against the charge. The relative widths were obtained in the following way. First the time profile of the pulse of ions entering the drift tube was deconvoluted from the measured peak profile, and then the width of the deconvoluted peak was divided by the width of the peak calculated for a single structural isomer with the transport equation for ions in the drift tube.[29] For the lowest charge states, the most folded conformations, the relative widths approach one. For the high charge states, the most unfolded conformations, the relative widths are also close to one. But for the intermediate charge states the peaks are broad, indicating the presence of many slightly-different conformations with comparable stabilities. Note the abrupt decrease in the relative widths that occurs between the +10 and +11 charge states.

The collision cross sections obtained for some of the conformations of apomyoglobin using eq 1 are plotted in Figure 6. Many of the features in the drift time distributions for apomyoglobin are poorly resolved. Figure 6 shows cross sections determined for the clearly resolved ones. The filled circles correspond to the features observed at high injection energies. The open circles correspond to metastable features which anneal into more stable ones at elevated injection energies. Only one folded conformation exists for the +4 charge state. Only one unfolded conformation is observed for high charge states. Multiple conformations are detected for intermediate charge states. There is a rather sharp structural transition at around the +7 charge state and the protein unfolds as the charge increases.

So far we have concentrated on the conformations of myoglobin devoid of the heme group. To see if the presence of the heme group has any profound influence on the conformations of gas-phase myoglobin, we have recorded drift time distributions for the +8 and +9 charge states of myoglobin

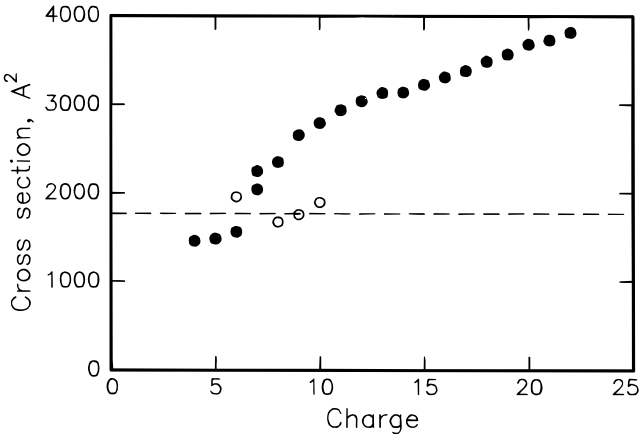

Figure 6. Measured collision cross sections for the resolved conformations of apomyoglobin plotted against the charge. Filled circles show the cross sections for the stable conformations. Open circles show the cross sections for metastable conformations which convert into stable ones when the injection energy is increased. The dashed line shows the cross section calculated for the native form of myoglobin using the exact hard spheres scattering model.

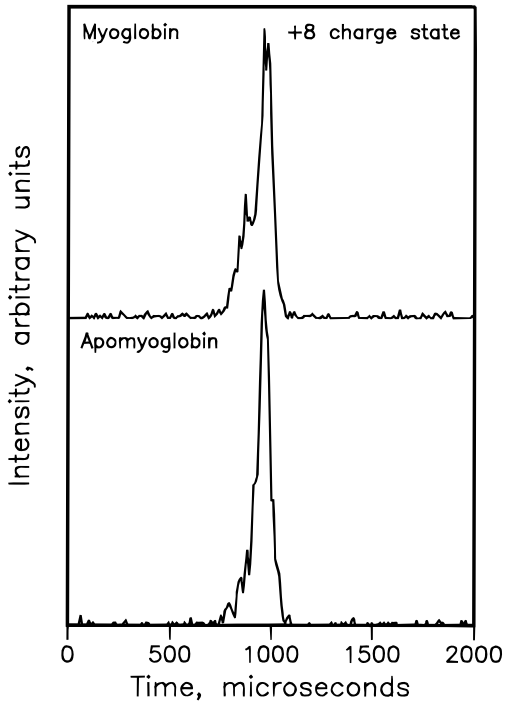

Figure 7. Drift time distributions recorded for the +8 charge states of myoglobin and apomyoglobin electrosprayed from a neutral solution. The injection energy was 1200 eV.

electrosprayed from a neutral (pH ≈7) solution. Figure 7 shows the drift time distributions for the +8 charge state of myoglobin and apomyoglobin recorded at an injection energy of 1200 eV. Under these conditions approximately half of the myoglobin ions have dissociated to apomyoglobin. Two features are present in the drift time distributions for both proteins. Both features occur at essentially the same drift time regardless of the presence of the heme. Thus it seems that similar conformations are present for myoglobin and apomyoglobin. The smaller feature at shorter drift times is more abundant for myoglobin. However, the smaller feature anneals into the larger one as the injection energy is increased (see Figure 2). The 1200 eV drift time distribution of myoglobin (Figure 7) is very similar to the 1000 eV drift time distribution of apomyoglobin (see Figure 2), where the feature at shorter drift times is more pronounced. It seems that the more compact structure is stabilized by the presence of the heme. A similar effect is observed in the drift time distributions for the +9 charge state. Thus the stabilization of more compact structures by the presence of the heme group seems to be a general phenomenon. Note that for these low charge states generated by direct electrospray ionization, the heme remains bound to myoglobin even when the protein is partially unfolded.

Discussion

Collins and Douglas have recently reported a study of the conformations of gas-phase myoglobin and apomyoglobin using the kinetic energy loss in ion beam scattering experiments.[16] They found that the collision cross sections for the +7 to +14 charge states systematically increase with charge and with the collision energy in the desolvation region. Both of these conclusions are supported by our results. The collision cross sections reported by Collins and Douglas are also in a reasonable quantitative agreement with our measurements. On the other hand, Collins and Douglas failed to resolve multiple conformations in their studies.

The compact conformations observed for the low charge states appear to be slightly more compact than the native protein. Globular proteins contain cavities large enough to accommodate water molecules and in solution the side chains extend into the solvent. In the absence of the solvent the protein should pack more tightly. Molecular dynamics simulations performed for BPTI indicate the radius of gyration decreases by 5% when the solvent is removed and by 8% on going from the crystal into vacuum.[41,42] Thus the observation of conformations slightly more compact than the native conformation is expected. However, while the conformations for the low charge states generated by gas-phase protein folding have cross sections close to that expected for a collapsed native conformation, this does not mean that they have this structure. The native conformation may be stable in the gas phase, but there are probably other more-stable conformations that are accessible kinetically.

In solution, acid denaturation of apomyoglobin proceeds through a compact "molten globule" intermediates to an unfolded state.[43] Circular dichroism spectra show that at pH =3 unfolding is almost complete and the unfolded state dominates, although the "molten globule" state is still present.[44] Our previous studies of cytochrome *c* suggest that part of the folded solution structure of a protein survives the electrospraying process.[23] Thus it is possible that the two peaks seen in the drift time distributions of the +8 to +10 charge states at low injection energies result from the two conformations of the protein present in solution at pH =3. The drift times of both conformations indicate that they are relatively compact. Thus unfolded solution conformations (as indicated by the circular dichroism spectra) produce partially folded gas-phase conformations. This may reflect the actual geometry of the unfolded conformations in solution or result from the spontaneous collapse of more extended structures in the gas phase (see below).

A number of distinguishable gas-phase conformations has been observed for apomyoglobin in the ion mobility measurements reported here. Conformations that are slightly more compact than the native form are preferred for lower charge states, and for higher charge states the preferred conformations are unfolded. This structural transformation probably results from Coulomb repulsion. For the lower charge states, Coulomb

(41) van Gunsteren, W. F.; Karplus, M. *Biochemistry* **1982**, *21*, 2259.
(42) Levitt, M.; Sharon, R. *Proc. Natl. Acad. Sci. U.S.A.* **1988**, *85*, 7557.
(43) Ohgushi, M.; Wada, A. *FEBS Lett.* **1983**, *164*, 21. Ptitsyn, O. B. *J. Protein Chem.* **1987**, *6*, 273. Kuwajima, K. *Proteins* **1989**, *6*, 87.
(44) Goto, Y.; Fink, A. L. *J. Mol. Biol.* **1990**, *214*, 803.

repulsion is not strong enough to overcome the intramolecular cohesive interactions, and the protein adopts a compact geometry where these interactions are maximized. For intermediate charge states, the increase in Coulomb repulsion probably results in the break-up of the compact conformation into a number of extended and folded domains. For the higher charge states, Coulomb repulsion should force the protein to adopt elongated geometries (see below), which are even less compact. For the low and high charge states, structural transformations occur with low activation barriers so that unstable conformations spontaneously unfold (or fold) into more stable ones. For intermediate charge states structural transformations occur with activation barriers, so that metastable intermediates become trapped and can be detected. The structural transition that occurs with increasing charge for apomyoglobin is somewhat analogous to acid denaturation of a protein in solution. A similar unfolding transition was observed for cytochrome *c*. However, for cytochrome *c* the unfolding transition occurs at slightly lower charge states, as expected for a smaller protein.

The peaks in the high-injection-energy drift time distributions for both the low and high charge states of apomyoglobin are narrow, with widths close to that expected for single geometries. This suggests that the protein may have a unique folded gas-phase conformation, or at least only a relatively small number of folded conformations with similar collision cross sections. For the high charge states the increase in Coulomb repulsion probably drives the adoption of an ordered string-like conformation, rather than random-coil-like conformations with a poorly defined structure. In contrast, the peaks for the intermediate charge states are very broad. Thus the unfolding transition observed as the protein charge increases (see the right-hand column in Figure 4) seems to proceed from an ordered folded structure to an ordered unfolded structure through a series of less-ordered intermediates.

While the cross sections for the extended conformations of the high charge states are significantly larger than expected for the native conformation, they are also significantly smaller than expected for an extended string, indicating that the extended conformations contain some folded domains or elements of secondary structure. In our discussion of possible structures for the extended conformations of cytochrome *c*[23] we argued that they were probably elongated geometries incorporating helical regions and intramolecular charge "solvation" shells. An α-helix is a favorable gas-phase conformation because it reduces Coulomb repulsion relative to a globular geometry, while the intramolecular cohesive free energy for an α-helix can be rather large, 16.7 kJ mol^{-1} per residue according to theoretical estimates.[6] On the other hand, in the absence of a solvent, intramolecular charge "solvation" becomes important and an α-helix is not effective in this regard. Thus the helical regions are probably disrupted by intramolecular charge solvation shells. The lowest energy conformation will be determined by a balance between attractive intramolecular interactions, intramolecular charge "solvation", and Coulomb repulsion. Elongated geometries are favored because of their lower Coulomb energy, and as the charge increases we suggested that the increase in the cross section that occurs results from the elongated geometry unraveling further to reduce the Coulomb energy. This unwinding ultimately results in formation of an extended polypeptide string, possibly with a higher residue density around charged sites due to intramolecular charge "solvation".

The formation and subsequent unwinding of an elongated conformation in response to an increase in the charge may be a universal phenomenon for protonated polypeptides. If this is true, the collision cross section of a polypeptide, normalized by dividing it by the number of residues, should be a universal function of the linear charge density on the polypeptide. Figure 8 shows the normalized collision cross sections for the most extended conformations of cytochrome *c* (+7 to +20 charge states) and apomyoglobin (+9 to +22 charge states) plotted against the charge density. The normalized cross sections for the two proteins fall on the same line, implying that their most extended conformations are structurally similar. The horizontal lines in the figure show the average scaled cross sections for the native, α-helix, and string-like forms of the two proteins. Cytochrome *c*, which has a higher density of basic residues than myoglobin, attains a higher charge density.

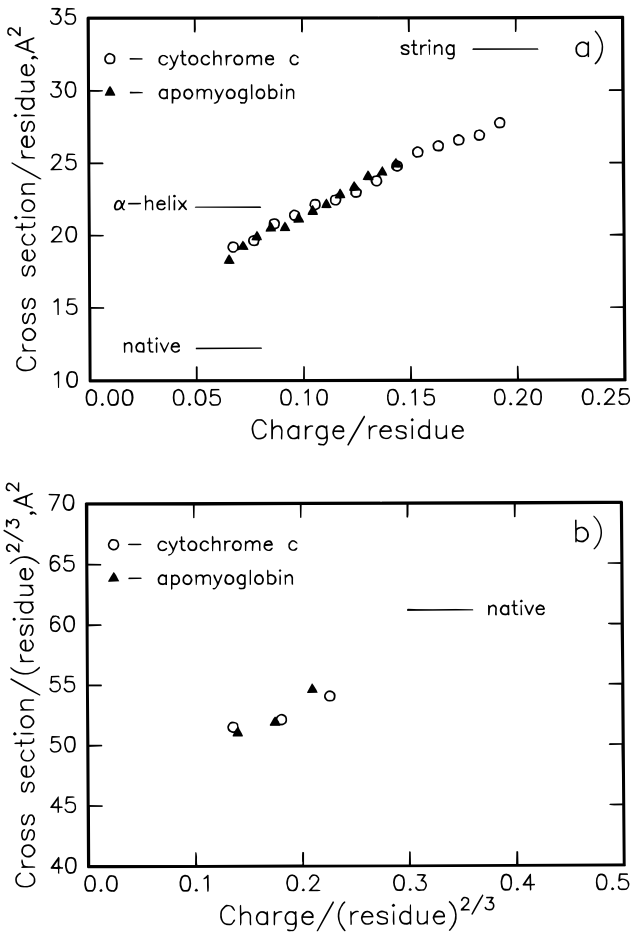

Figure 8. The scaled collision cross sections of (a) the extended conformations of apomyoglobin and cytochrome *c* and (b) the folded conformations of these proteins as a function of charge density. For the extended conformations, which are believed to be roughly linear, the normalized cross sections and charge densities were obtained by dividing the measured cross sections and charge by the number of residues. For the folded conformations which are roughly spherical, the normalization was performed by dividing the cross section and charge by the number of residues to the $^2/_3$ power. The horizontal lines correspond to the average scaled collision cross sections calculated for native, α-helical, and string-like conformations using the exact hard spheres scattering model.

The packing densities of the most compact conformations of cytochrome *c* and apomyoglobin are close to those of the native proteins in solution (see Figure 6). Native cytochrome *c* and myoglobin have very similar packing densities. Therefore the packing densities of the two gas-phase proteins must also be similar. Figure 8b compares the normalized cross sections of the most compact conformations of cytochrome *c* and apomyoglobin as a function of the surface charge density. The compact conformations are assumed to have geometries close to spherical, so that both the collision cross section and the surface charge

density are proportional to the number of residues to the $^2/_3$ power. The normalized cross sections of the low charge states of the two proteins are nearly identical. In solution, the similarity in the packing densities of most globular proteins arises from similarities in their structures, such as the presence of a tightly packed hydrophobic core and common secondary structure elements. The similarity in the packing densities of the compact conformations of gas-phase proteins may also imply a structural similarity. For example, secondary structure is likely to exist in compact gas-phase proteins as well, and the core of hydrophobic residues may be replaced by a core of polar residues.[45] The cross sections of the most compact conformation increase slightly with charge, presumably in response to the increase in Coulomb repulsion.

For the intermediate charge states, comparison of the collision cross sections of apomyoglobin and cytochrome *c* is less straightforward. These conformations are intermediates in the transition from compact three-dimensional structures to one-dimensional structures. At a given charge density, the intermediate conformations of apomyoglobin tend to be less compact than those of cytochrome *c*. This may result from the fact that cytochrome *c* has a higher fraction of polar residues than myoglobin (0.56 versus 0.49) and thus it can form compact intermediates with a higher density of polar−polar contacts. Since the larger Coulomb repulsion in compact conformations must be balanced by the intramolecular cohesive energy, cytochrome *c* can form more compact intermediates at a given charge density than apomyoglobin.

Conformations almost as compact as the native form are not formed as a direct result of the collapse of extended structures upon proton stripping (see Figure 4). Instead, the collapse results in formation of partially-folded structures which, when collisionally heated, isomerize into compact conformations. Thus protein folding *in vacuo* proceeds with an activation barrier. This barrier probably arises because structural rearrangements into more compact structures are opposed by Coulomb repulsion. Indeed, the height of the barrier seems to decrease with charge. For example, at 750 eV injection energy the compact conformation accounts for only about 27% of the isomer distribution for the +6 charge state (see Figure 3), but it accounts for 70% for the +5 charge state. The origin of the Coulomb barrier to gas-phase protein folding can be readily understood: On going from an extended conformation to a folded conformation the Coulomb energy increases before it can be offset by the shorter-range intramolecular interactions which hold the protein in a folded conformation. In solution the Coulomb barrier will be reduced by the high dielectric constant of water. An additional contribution to the activation barrier for protein folding in the gas phase could result from the rearrangement of secondary structure domains, which are likely to be the major structural component in partially-folded proteins, into an ordered compact structure. Such a rearrangement may require the unzipping of a portion of the secondary structure, giving rise to an activation barrier. For cytochrome *c*, collapsed structures generated by proton stripping of higher charge states also become more compact when collisionally annealed. However, the changes were much smaller than observed for the +6 charge state of apomyoglobin, and could result mainly from the ordering of a disordered structure generated in the initial collapse following proton stripping.[24] However, it appears that the presence of activation barriers for gas-phase protein folding is a general phenomenon.

(45) Wolynes, P. G. *Proc. Natl. Acad. Sci. U.S.A.* **1995**, *92*, 2426.

Conclusions

A wide variety of conformations have been observed for apomyoglobin ions in the gas phase. Partially-folded structures, which can be produced for intermediate charge states by direct electrospray ionization, unfold into more extended conformations when collisionally heated. The extended conformations appear to be the preferred gas-phase conformation for intermediate and high charge states. Comparison of the measured cross sections with the cross section calculated for the native conformation suggests that the preferred gas-phase conformations of the lower charge states are slightly more compact than the native form. Thus as the charge increases, apomyoglobin undergoes an unfolding transition that is driven by Coulomb repulsion. The cross sections per residue of the extended conformations of apomyoglobin and cytochrome *c* scale with the charge per residue, as do the cross sections for the compact folded conformations of these proteins. This suggests that the extended and folded conformations for different proteins share common structural motifs in the gas phase.

When the lower charge states are produced by proton stripping from unfolded, higher-charge states they spontaneously collapse into partially-folded structures. The collapsed structures become more compact when collisionally heated. This result indicates that there is an activation barrier for the folding of apomyoglobin in the gas phase. The presence of an activation barrier for gas-phase protein folding appears to be a general phenomenon. The barrier probably results from Coulomb repulsion and the reorganization of secondary structure. Folding intermediates were observed for some charge states of apomyoglobin. It appears that folding proceeds through a series of similarly-shaped intermediates that become increasingly compact rather than through several distinct structural rearrangements involving well-defined intermediates.

Acknowledgment. We gratefully acknowledge the National Science Foundation (Grant No. CHE-9306900) for partial support of this work.

JA962914K